ResearchGate

See discussions, stats, and author profiles for this publication at: https://www.researchgate.net/publication/316969624

Evaluation of performance of silicon photomultipliers in lidar applications

Conference Paper · May 2017

DOI: 10.1117/12.2264935

CITATIONS
15

READS
1,256

1 author:

Sergey Vinogradov
Lebedev Physical Institute, Russian Academy of Sciences

60 PUBLICATIONS **535** CITATIONS

SEE PROFILE

All content following this page was uploaded by Sergey Vinogradov on 23 February 2018.

The user has requested enhancement of the downloaded file.

Ouster Exhibit 2012
IPR2023-01457 - Page 001

Evaluation of performance of silicon photomultipliers in LIDAR applications

Sergey. L. Vinogradov*[a,b,c]
[a]P.N. Lebedev Physical Institute of the Russian Academy of Sciences, Moscow, 119991, Russia
[b]National Research Nuclear University "MEPhI", Moscow, 115409, Russia
[c]University of Liverpool, Sci-Tech Daresbury, Warrington WA4 4AD, UK

ABSTRACT

Silicon Photomultipliers (SiPMs) are a well-recognized new generation of photon number resolving avalanche photodetectors. Many advantages – a high gain with an ultra-low excess noise of multiplication, multi-pixel architecture, relatively low operating voltage – make SiPMs very competitive in a growing number of applications. Challenging demands of LIDAR applications for a receiver having high sensitivity starting from single photons, superior time-of-flight resolution, robustness including surviving at bright light flashes, solid-state compactness and more, are expected to be feasible for the SiPMs. Despite some known drawbacks, namely crosstalk, afterpulsing, dark noise, limited dynamic range, SiPMs are already considered as promising substitutes for conventional APDs and PMTs in LIDAR applications. However, these initial considerations are based on a rather simplified representation of the SiPM as a generic LIDAR receiver described by generic expressions.

This study is focused on a comprehensive evaluation of a SiPM potential considering essential features of this new technology, which could affect applicability and performance of SiPMs as LIDAR receivers. Namely, an excess noise due to correlated processes of crosstalk and afterpulsing, are included into account utilizing the well-established framework of analytical probabilistic models. The analysis of SiPM performance in terms of a photon number and time resolution clarifies their competitiveness over conventional APD and PMT and anticipates the development of next SiPM generations.

Keywords: silicon photomultiplier, SiPM, LIDAR, SNR, time resolution, analytical model

1. INTRODUCTION

Nowadays a SiPM is a well-established new generation of photodetectors widely recognized due to their unique advantages with respect to conventional PMT, linear mode APD, and Geiger mode APD in photon number resolving detection of low-level light pulses. An initial SiPM generation has been developed in Russia starting from basic research of an avalanche breakdown with negative feedback in Metal-Insulator-Semiconductor structures in 1970s-1980s [1-2], R&D of Metal-Resistor-Semiconductor structures as operational SiPM prototypes in 1980s-1990s [3-5], and development of the most feasible, reliable, efficient and thus popular design of a modern conventional SiPM as a matrix of independent GM APD cells with polysilicon quenching resistors with common output in 2000s [6-7]. Some more details on the R&D of SiPMs could be found elsewhere, for example, the author's point of view is expressed in [8].

Most of the SiPM application studies during the 2000s were focused on a detection of scintillation and Cherenkov light pulses in high energy particle physics, astrophysics, and nuclear medicine, especially positron emission tomography, as discussed in [6-7] and [9]. However, the feasibility of a LIDAR receiver based on SiPM technology has been undisclosed till the 2010s, even if some SiPM developers (SensL, Amplification Technologies) mentioned LIDAR as a target application for their SiPMs on the corporate web pages much earlier. So, this application area is rather new, and just a few papers reported on studies in it as discussed below.

To the best of author's knowledge, first experimental studies on SiPM feasibility as a LIDAR receiver have been started

*vin@lebedev.ru; phone +7 499 132-6286; www.lebedev.ru

Photon Counting Applications 2017, edited by Ivan Prochazka, Roman Sobolewski, Ralph B. James, Proc. of SPIE Vol. 10229, 102290L · © 2017 SPIE · CCC code: 0277-786X/17/$18 · doi: 10.1117/12.2264935

Ouster Exhibit 2012
IPR2023-01457 - Page 002

Downloaded From: http://proceedings.spiedigitallibrary.org/ on 05/24/2017 Terms of Use: http://spiedigitallibrary.org/ss/termsofuse.aspx

in 2010. 3D airborne topographic mapping with SiPM samples from Amplification Technologies has been evaluated by Optech (now Teledyne Optech) and analyzed by the author: dynamic nonlinearity of SiPM response due to a limited number of pixels and long pixel recovery time has been identified as a major drawback in the detection of multiple reflections [10]. Feasibility of a multiple-target laser rangefinding using a 4x4 SiPM array of 2.85x2.85 mm^2 samples from SensL was investigated in a wide range of operating condition (from 16 photons per pulse to saturation, from 50 ns to 500 ns laser pulse width). The authors emphasized superior sensitivity of the SiPM approaching to a quantum limit of detection (single photoelectron count), noted considerable nonlinearity of the SiPM responsivity, and obtained an accuracy of the rangefinding of 15 cm for the range of 10 m [11].

SiPM for atmospheric lidar applications has been studied for the first time in [12], where SiPM (Hamamatsu MPPC S10362-33-100C, 3x3 mm^2; 900 pixels) has been directly compared with conventional PMT (Hamamatsu R7400P). The authors were satisfied with SiPM behavior even with some dead time nonlinearity and concluded that SiPM is suitable for elastic-backscatter aerosol lidars. The SiPM performance in SNR has been evaluated of about 2.3 times better than that of the PMT in a signal shot-noise dominated regime at low altitude and about 1.7 times worse in a photoreceiver-noise dominated regime due to much higher dark count rate (DCR) of SiPM. This study was advanced in more details comparing the same Hamamatsu MPPC and PMT also with SensL SiPM 30035 as well as applying specific formalism to the SNR expressions [13]. In fact, the formalism coincides with a probabilistic approach based on a random number of counts where the signal is associated with a mean, and the noise is associated with a standard deviation of corresponding random variables. All specific features of the contenders were considered just as two parameters: photon detection efficiency η and excess noise factor F, and the authors found that SNR performance is better for detectors with higher η/F values (accordingly to values provided in the paper, #1 - MPPC, #2 - PMT, #3 - SiPM). The same formalism was reproduced and discussed with respect to the photodetectors potential and competitiveness in general also in [14].

Experimental comparison of SiPM (STMicroelectronics SPM42H6-60P, 3.96 x 4.44 mm^2, 4871 pixels) and linear mode Si-APD Laser Components SAR500H4 (0.5 mm diameter) has been reported in [15]. The authors observed the much higher performance of SiPM in a variety of experimental conditions: the ratio of SNR for SiPM to SNR for APD was 1300:180 in the indoor detection in a range of 36 m, and 300:8 in the sunny outdoor detection (high background illumination) in the same range.

A few more publications also described some general considerations of SiPM advantages and features with respect to LIDAR application supported by some experimental results [16-17].

There were several studies on the performance of a single element SPAD as a super-sensitive alternative to a linear mode APD [18-19]. However, the well-known disadvantage of the SPAD in the inability to measure an amplitude of reflected signals appears to be of critical importance in some cases, and even being able to recover multi-reflection features from time-of-flight (TOF) statistics histograms, SPAD-based LIDARs are not applicable for a single shot operation.

In contrast, a 2D SPAD array/matrix could be applicable for a photon number resolving detection and it is considered as potentially an ideal photon detector due to the ability to readout every photon count timestamp asynchronously and independently due to direct access to every single SPAD in the array. Regretfully, even mature CMOS technology does not resolve a problem of a low fill factor (ratio of sensitive area to the total area occupied by electronics for active quenching of Geiger discharge) of the front-side SPAD arrays. For example, the recent development of MiSPIA (Microelectronic Single-Photon 3D Imaging Array) carried out by the world-recognized leaders in R&D of SPADs (Politecnico di Milano, Micro Photon Devices, Fraunhofer IMS) resulted in the fill factor of 3.14% for the 150 μm pitch 30 μm active area FrontSPAD array [20-21]. Regretfully, an attempt to eliminate the fill-factor problem by using backside illuminated SPAD technology with SOI substrate introduced prohibitively high dark count rate (DCR) of about 240 Kcps for a single pixel of the 150 μm pitch 143 μm active area BackSPAD array with the fill factor of 71.4% (about 40 times higher than DCR for the FrontSPAD. The better result (fill factor of 20% for the front-side SPAD array of 4x32 SPADs – so-called digital SiPM, dSiPM) has been reported by partially the same team (Politecnico di Milano, Micro Photon Devices) a year later [22].

Another approach to a SPAD array design has been demonstrated by Philips in their digital SiPM (dSiPM), where a direct access is provided to a sub-group of SPADs (sub-pixels of dSiPM) to reduce the number of electronic components and connections at the front-side area [23]. The fill factor of the dSiPM initially was achieved at the level of 50% (pixel size of 52 μm × 30 μm), i.e. about comparable with conventional analog SiPMs which fill factor is in a range of 30% - 80% depending on a pixel size. In the recent optimization of the dSiPM, the fill factor has been improved to 78% (pixel size of

Ouster Exhibit 2012
IPR2023-01457 - Page 003
Downloaded From: http://proceedings.spiedigitallibrary.org/ on 05/24/2017 Terms of Use: http://spiedigitallibrary.org/ss/termsofuse.aspx

59.4μm x 64μm) [24]. However, dSiPM technology is rather expensive and inflexible in scaling of the dSiPM dimensions and especially in producing arrays of dSiPMs due to large periphery occupied by electronics.

Therefore, to the best of the author's knowledge, there are no attempts either to implement SPAD arrays or dSiPMs as a single photon number resolving LIDAR receiver or to combine an array of SPAD arrays or dSiPMs as a focal plane array of photon number resolving detectors in 3D imaging LIDARs. In this situation, detailed analysis of the SPAD-based receivers is out of the scope of this paper.

2. FILTERED MARKED POINT PROCESS MODELING

2.1 Model statements and expressions

Let us start with metrics of the LIDAR receiver performance just referencing to the following statement from the paper [11]: "*Two most important performance indicators of a rangefinder are "range" and "range resolution." The "range" is the maximum distance that can be measured. It is dictated by the system loss budget and the reflectance of the target... The range resolution is usually determined by the rise time of the returned pulse after it is detected by the receiver*." Obviously, the maximum range is determined by a detector *SNR* or, inversely, by a noise-to-signal ratio *NS*R or signal resolution *SR*, and the range resolution is determined by a detector time resolution *TR*. Even though both SNR and TR are essential indicators, many comparative studies and performance analyses of LIDAR receivers are exclusively focused on SNR (for example, [12-14]). In case if TR is considered, it is associated with some rise time which is roughly determined either by a readout electronics frequency bandwidth or by a laser pulse temporal profile.

In contrast, most of the studies related to TOF applications of scintillation detectors in high energy physics and nuclear medicine (TOF-PET) comprehensively consider temporal profiles of every process involved in the formation of an output signal (e.g. [25-29]). Thus, it seems to be useful to apply well-established approaches of scintillation detection modeling to LIDAR application of SiPM in a combined SNR and TR analysis.

An output signal represents a stochastic process which can be characterized at any time point as a random variable having some probability distribution with specific mean (expectation) and variance values. In correspondence with the basic statements with respect to the stochastic process in scintillation detectors and photodetectors [30-31], an output signal is a filtered marked point process. Implementation of results [30-31] based on the development of probabilistic SiPM response models taking into account SiPM-specific effects: correlated noise (crosstalk and afterpulsing) and nonlinearity (binomial distribution of fired pixels and recovery time-related statistics) have been carried out in [32-36]. Results of these studies are used in this paper and summarized below.

So, an arbitrary stochastic output signal process $s(t)$ has a mean function $\mu_s(t)$ and a variance function $\sigma_s^2(t)$ with some additive noise having zero mean and stationary variance σ_n^2, hence, the output signal resolution $SR(t)$ and time resolution $TR(t)$ are defined as explicit deterministic functions of time t:

$$SR = NSR = 1/SNR = \frac{\sqrt{\sigma_s^{\ 2} + \sigma_n^{\ 2}}}{\mu_s} \tag{1}$$

$$TR = \frac{\sqrt{\sigma_s^{\ 2} + \sigma_n^{\ 2}}}{\frac{d\mu_s}{dt}} \tag{2}$$

Expression (2) corresponds to the most common cases of leading edge discriminator and constant fraction discriminator detections of the signal arrival time. Let us turn to a common measure of output signals as a voltage signals $V_{out}(t)$ for practical clarity and then express mean and variance functions in the voltage units:

$$\mu_s\ (t) = E[V_{out}(t)]\ ; \qquad \sigma_s^2(t) = Var[V_{out}(t)] \tag{3}$$

Ouster Exhibit 2012
IPR2023-01457 - Page 004
Downloaded From: http://proceedings.spiedigitallibrary.org/ on 05/24/2017 Terms of Use: http://spiedigitallibrary.org/ss/termsofuse.aspx

$$
\begin{aligned}
&E[V_{out}(t)] = \overline{N}_{pe} \cdot (1+\overline{K}_{\sec}) \cdot [\rho_{tot} * h](t) \\
&Var[V_{out}(t)] = ENF_{gain} \cdot (1+\overline{K}_{\sec})^2 \cdot ENF_{\sec} \cdot \overline{N}_{pe} \cdot [\rho_{tot} * h^2](t) \\
&\rho_{tot}(t) = [\rho_{ph} * \rho_{sptr} * \rho_{\sec}](t) \\
&ENF_{gain} = 1 + \frac{Var[Gain]}{Gain^2} \\
&ENF_{\sec} = 1 + \frac{Var[K_{\sec}]}{\overline{K}_{\sec}^2}
\end{aligned}
\tag{4}
$$

Where N_{pe} is a Poisson distributed number of photoelectrons per light pulse, ρ_{ph} is a probability density function of photon arrival times, ρ_{sptr} is a probability density function of a single photon time detections (time jitter, SPTR), V_{ser} is an amplitude of a single electron response (SER), ENF_{gain} is an excess noise factor of a charge multiplication gain with the mean value *Gain*, and ENF_{sec} is an excess noise factor of correlated (secondary) events – crosstalk and afterpulsing with mean number of events – K_{sec} (more details on correlated events statistics could be found in [37]).

Noise contributions to the σ_n^2 in (1) and (2) are related to stationary filtered stochastic counting process of dark *(DCR*) and background (*BCR*) events resulted in a baseline fluctuations as well as to stationary noise of the electronic readout circuitry σ_{el}^2:

$$\sigma_n^2 = (DCR + BCR) \cdot ENF_{gain} \cdot ENF_{sec} \cdot (1 + K_{sec})^2 \int_0^\infty h(t)^2 dt + \sigma_{el}^2 \tag{5}$$

2.2 Model assumptions

Assumptions on temporal shapes of the probability density functions and photodetector responses, signal, and noise parameters are as follows:

ρ_{ph} and ρ_{sptr} obey normal distributions (as typically assumed in modelling and measured in experiments, see e.g. [38], [35-36]) with standard deviations S_{ph} and S_{sptr} correspondingly, so their convolution is the normal distribution again which corresponds to the photon detection time distribution with standard deviation S_{tts} (mean of the distribution is set to zero for simplicity):

$$S_{tts} = \sqrt{S_{ph}^2 + S_{sptr}^2} \tag{6}$$

ρ_{sec} is assumed to be a Dirac delta function to simplify considerations and preserve analytical clarity of the model results because in this study we are not exclusively focused on the timing of correlated events. Nevertheless, a total impact from crosstalk and afterpulsing noises is taken into account by ENF_{sec}.

SER temporal profile *h(t)* of the photodetector (filter function) is modeled by a bi-exponential function with the amplitude $V_{ser}(Gain) \sim Gain$ and $\sim R$ (preamplifier load resistance), rise time T_r and decay time T_d:

$$h(t) = V_{ser}(Gain) \cdot \left(e^{-\frac{t}{Tr}} - e^{-\frac{t}{Td}}\right) \tag{7}$$

$$V_{ser}(Gain) = \frac{q \cdot Gain \cdot R}{Td - Tr} \tag{8}$$

In this case considering contribution from dark and background noise counts (5) the integral term in (5) is

$$\int_0^\infty h(t)^2 dt = \frac{(q \cdot Gain \cdot R)^2}{2 \cdot (Td + Tr)} \tag{9}$$

σ_{el}^2 is assumed to be a standard deviation of the additive white Gaussian noise (AWGN) defined by thermal noise at R=50 Ohm at room temperature in the bandwidth of 1 GHz. However, this rough marginal estimate results in a noise of ~ 30 μV, which is about 10 times lower than specifications of input noise of the popular digital scopes

Ouster Exhibit 2012
IPR2023-01457 - Page 005
Downloaded From: http://proceedings.spiedigitallibrary.org/ on 05/24/2017 Terms of Use: http://spiedigitallibrary.org/ss/termsofuse.aspx

(true RMS of 230 – 550 μV in a true 1 GHz BW as discussed in [39]); it should be adjusted for actual parameters of the readout electronics depending on an application-specific optimisation.

2.3 Model results

Model results are presented for two distinct cases of laser pulse width. First, for much shorter than any SiPM characteristic times, namely SPTR, and SER rise time, particularly, 40 ps FWHM as it corresponds to our experimental studies [34] discussed below in section 3. Second, for much longer laser pulse width than that times, particularly, 10 ns FWHM as it corresponds to some typical LIDAR specifications.

Main timing functions responsible for SNR and TR are presented in Figure 1 as expressed by (1-4): Gaussian distribution with sigma S_{tts} (6) of photon detection or avalanche triggering times (TTS) is convolved with the SER pulse shape $h(t)$ (7) producing mean output signal (Mean). The TTS convolved with squared SER $h(t)^2$ yields the variance and standard deviation (StdDev) of the signal.

Figure 2 shows SNR and TR dependence on time when the signal mean and standard deviation is measured, i.e. in their dynamics. In the case of the short laser pulse (Fig. 2 a), the output signal has a slightly "blurred" bi-exponential shape, the minimal TR is achieved at about 10% of the Mean. In the case of long laser pulse when the output signal shape is strongly influenced by both TTS and SER, the minimal TR is achieved at about 30% of the Mean. It is a clear tendency defined by a position of the maximum of the mean signal derivative (from mean = 0 for a bi-exponential function to mean = 50% of the maximum signal for Gaussian function).

Two physical limits of photon detection performance are also shown in Figure 2 as reference lines SNR limit and TR limit. The SNR limit is defined as SNR of an ideal photon detector which has the same SNR as an incident photon pulse. As far as the number of incident photons N_{ph} obeys Poisson distribution, the SNR limit is as follows:

$$SNR_{limit} = \frac{E[N_{ph}]}{\sqrt{Var[N_{ph}]}} = \sqrt{N_{ph}} \tag{10}$$

The TR limit is defined as the Cramer- Rao lower bound (CRLB) of the laser pulse arrival time estimate using Fisher information integral [27]. CRLB is an ultimate time resolution achievable with an ideal photon detector in terms of SNR and timing [28]. As far as a reflected laser pulse is assumed to be Gaussian, the TR limit is as follows:

$$TR_{limit} = \frac{1}{\sqrt{N_{ph} \cdot \int_{-\infty}^{\infty} \left(\frac{dlog(\rho_{ph}(t))}{dt} \right)^2 \rho_{ph}(t) dt}} = \frac{S_{ph}}{\sqrt{N_{ph}}} \tag{11}$$

To observe a full range of achievable TR and SNR values in a single shot measurement of a reflected laser pulse, the dynamical TR vs dynamical SNR plots are presented in Figure 3 for competitive photodetectors: the SiPM of the same parameters as used for Figure 1 and 2, and for conventional APD and PMT having some typical parameters (see Figure 3 caption for details). It should be noted that APD in this case is assumed to be unable to detect the optical pulse of 100 photons because the SNR is below 1.

Ouster Exhibit 2012
IPR2023-01457 - Page 006
Downloaded From: http://proceedings.spiedigitallibrary.org/ on 05/24/2017 Terms of Use: http://spiedigitallibrary.org/ss/termsofuse.aspx

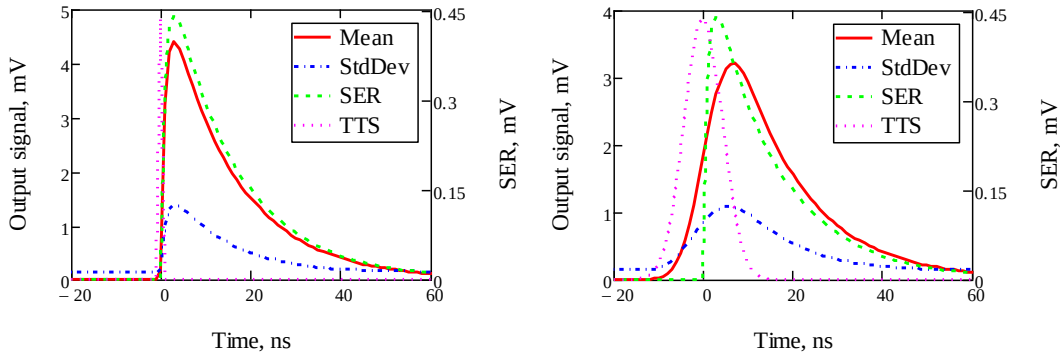

a) b)

Figure 1. Examples of SiPM output signals and instrumental responses: a) short laser pulse detection (40 ps FWHM); b) long laser pulse detection (10 ns FWHM). Parameters of the model are in partial correspondence with the experiment [34]: SiPM: S_{sptr} = 147 ps FWHM, Tr = 0.5 ns, Td = 15 ns, $Gain$ = 10^6, ENF_{gain}=1.01, DCR = 100 Kcps, PDE = 50%, ENF_{sec}=1.1 (i.e. probabilities of crosstalk and afterpulsing are less than about 10%);

Laser: Gaussian pulse with sigma S_{ph} of 40 ps (a) and 10 ns (b) FWHM, mean number of photons per pulse = 20;

Noise: background count rate BCR = 10 Mcps, electronic noise =30 μV (assumed to be equal to thermal noise at 50 Ohm in 1 GHz BW at room temperature, signal and noise values are given at the SiPM output / preamplifier input).

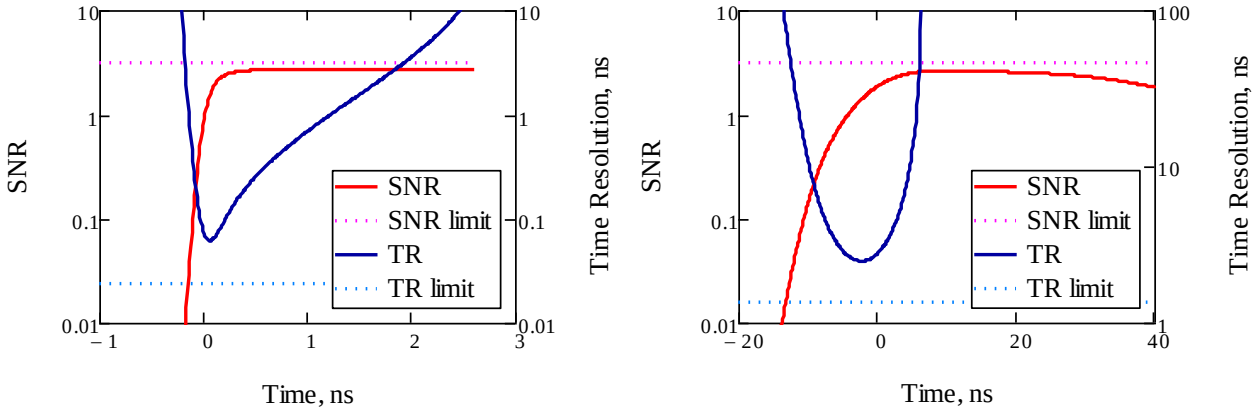

a) b)

Figure 2. Examples of dynamical SNR and TR (standard deviation) of SiPM output signals: a) short laser pulse detection (40 ps FWHM); b) long laser pulse detection (10 ns FWHM). Parameters of the model are the same as in Figure 1. Note much better TR and shorter time scale of plots in Fig. 1 a) with respect to other plots in Fig. 1 and 2.

Ouster Exhibit 2012
IPR2023-01457 - Page 007
Downloaded From: http://proceedings.spiedigitallibrary.org/ on 05/24/2017 Terms of Use: http://spiedigitallibrary.org/ss/termsofuse.aspx

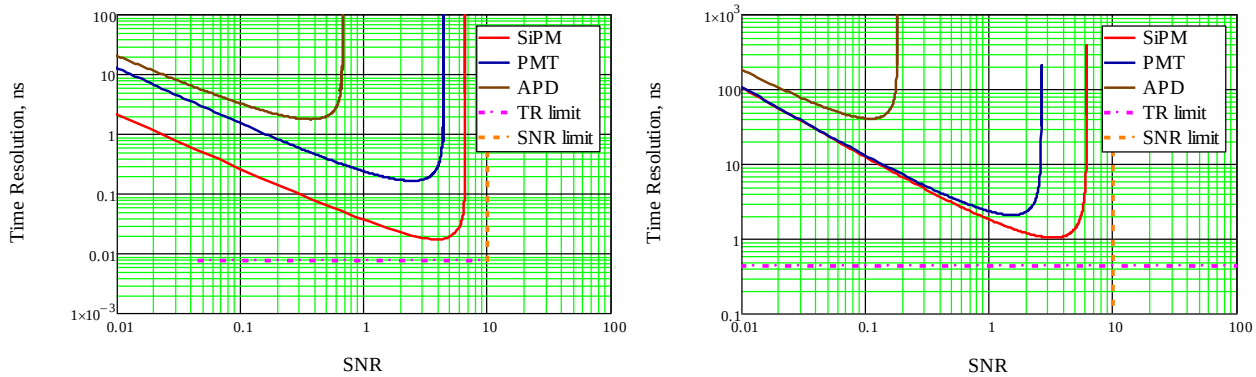

a) b)

Figure 3. Comparative examples of dynamical SNR and TR (standard deviation) of competitive photodetectors: a) short laser pulse detection (40 ps FWHM); b) long laser pulse detection (10 ns FWHM). Parameters of the model for SiPM, background and electronic noises are the same as in Figure 1; laser pulse of 100 photons. Parameters for APD and PMT are as follows:

APD: S_{sptr} = 0.5 ns, Tr = 0.5 ns, Td = 1.5 ns, $Gain$ = 10^2, ENF_{gain}=3, DCR = 100 Kcps, PDE = 75%, ENF_{sec}=1.0;

PMT: S_{sptr} = 0.5 ns, Tr = 0.5 ns, Td = 1 ns, $Gain$ = 10^6, ENF_{gain}=1.2, DCR = 100 cps, PDE = 25%, ENF_{sec}=1.0.

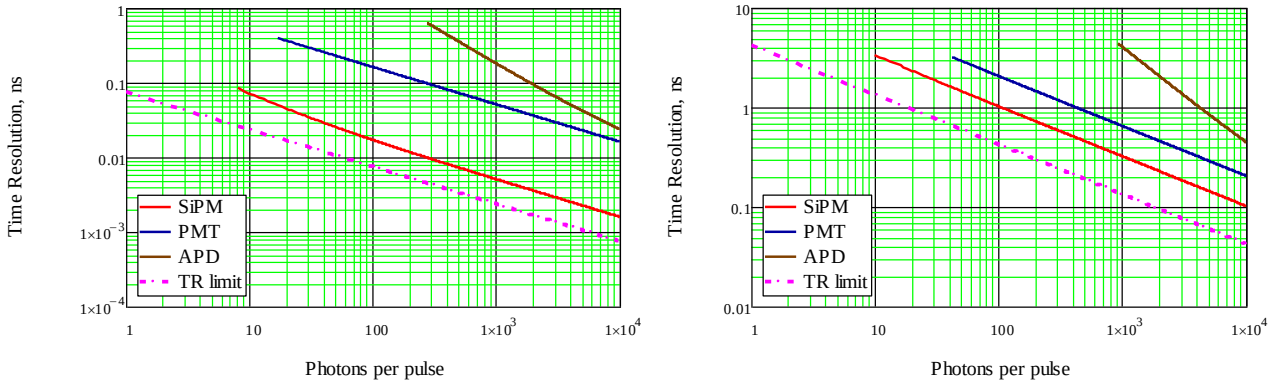

a) b)

Figure 4. Comparative examples of minimal achievable TR (standard deviation) of competitive photodetectors vs a number of photons per pulse N_{ph}: a) short laser pulse detection (40 ps FWHM); b) long laser pulse detection (10 ns FWHM). Parameters of the model are the same as in Figure 3. All plots of the TR are started with the threshold number of photons defined by $SNR(N_{ph})$ = 1 because at the lower N_{ph} the optical pulses could not be detected and the TR is undefined.

3. EXPERIMENTAL STUDIES

Initial experimental studies of SiPM TR in the case of a multi-photon short Gaussian laser pulse of 40 ps FWHM width have been carried out in [35-36], and their results are utilized in this paper for comparison with the model. Specific optimization of the SiPM readout resulted in improvement of the SER pulse shape reducing Td down to 1 ns, which is favorable for DCR noise and corresponding baseline fluctuation reduction as shown in Figure 5 a). SPTR of the device under test was also measured and found to be at the record level for the 3x3 mm^2 analog SiPM samples as shown in Figure 5 b).

Ouster Exhibit 2012
IPR2023-01457 - Page 008
Downloaded From: http://proceedings.spiedigitallibrary.org/ on 05/24/2017 Terms of Use: http://spiedigitallibrary.org/ss/termsofuse.aspx

Experimental results of multi-photon measurements of TR dependence on a number of photons per pulse N_{ph} (explicitly defined by measured N_{pe}) are shown in Figure 6. Experimental and model results on $TR(N_{pe})$ are in a good agreement in an appropriate range of N_{pe}. However, TR at high N_{pe} is limited by a fixed jitter of laser and electronics, which has not been extracted from the results. And at low $N_{pe} < 1$ the TR deviates from a simple expression (11) because of random losses of detections due to non-negligible probability to get zero detection event, which has not been included in the CRLB model. Such a correction of the CRLB model has been discussed and derived by S. Seifert et al. ([27], Appendix (A3)), and it actually improves its agreement with the experiment.

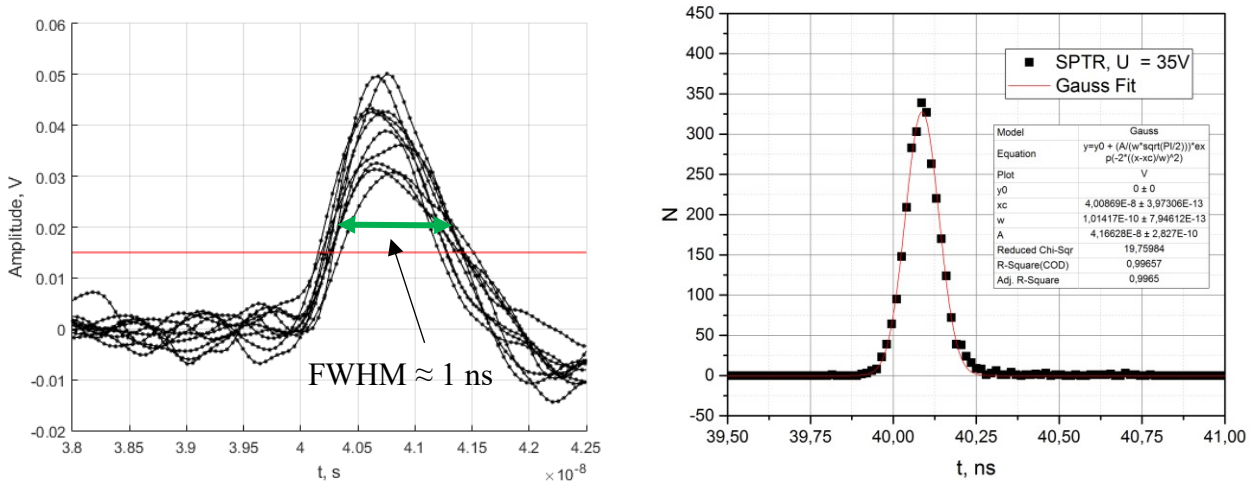

Figure 5. SiPM timing characteristics: a) SER, FWHM ≈ 1ns (Uov=4.5 V), b) SPTR, FWHM ≈ 119 ps (Uov=9.5 V).

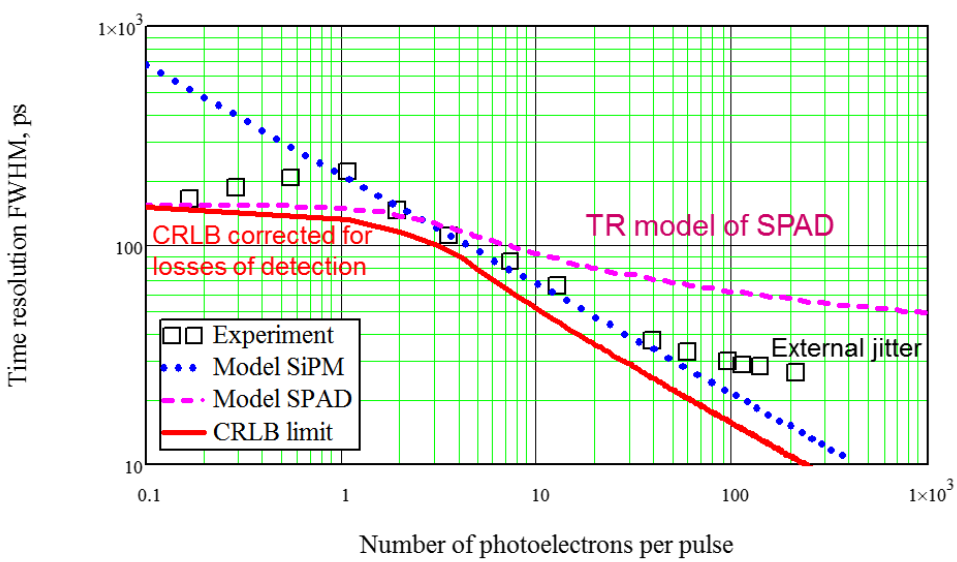

Figure 6. The time resolution of short laser pulse vs N_{pe} for the advanced analog 3x3 mm^2 KETEK SiPM: experiment and SiPM model as discussed above. SPAD model is based on order statistics of the first photon detection time as discussed in [37]. CRLB limit in case of a random number of photons as discussed in [27], Appendix (A3) is additionally corrected for probability of zero photons per pulse $N_{ph}=0$.

Ouster Exhibit 2012
IPR2023-01457 - Page 009
Downloaded From: http://proceedings.spiedigitallibrary.org/ on 05/24/2017 Terms of Use: http://spiedigitallibrary.org/ss/termsofuse.aspx

4. CONCLUSION

SiPM performance in SNR and time resolution has been evaluated using the theoretical framework of filtered marked point processes. Model results are in a good agreement with some preliminary experimental data for short multi-photon laser pulse detection. Definitely, these initial results require more comprehensive experimental studies and modeling, especially because such specific effects as a nonlinearity of an output SiPM response due to a limited number of pixels, a dependence of pixel recovery dynamics on incident light intensity, and dynamics of correlated processes (crosstalk and afterpulsing) have not been considered yet.

The analysis clarifies SiPM competitiveness over conventional APD and PMT as a 3D flash LIDAR receiver and anticipates the development of the next SiPM generations with a higher photon detection efficiency, higher density of pixels, faster pixel recovery, and shorter single electron response.

ACKNOWLEDGEMENTS

This work has been supported in part by the EC under Grant Agreement 329100 “SiPM in-depth”, by the Megagrant program of Russia under Grant Agreement 14.A12.31.0006 with the additional agreement №2 from 03.03.2016, and by the Russian Ministry of Education and Science under Contract 3.2989.2017.

This article is based upon work in Fast Advanced Scintillator Timing (FAST COST TD1401) action supported by COST (European Cooperation in Science and Technology).

REFERENCES

[1] Kravchenko A.B., Plotnikov A.F., and Shubin V.E. "Feasibility of construction of a pulsed avalanche photodetector based on MIS structure with stable internal amplification," Sov. J. Quantum Electron. 8, 1086 (1978).

[2] Kravchenko A.B., Plotnikov A.F., Popov Yu.M., and Shubin V.E., "Detection of light with an MIS structure operating under avalanche multiplication conditions," Sov. J. Quantum Electron. 11, 473 (1981).

[3] Gasanov A., Golovin V., Sadygov Z., and Yusipov N., Technical Physics Letters, v.14, No.8, p.706 (1988).

[4] Sadygov Z.Y. et al, "The investigation of possibility to create the multichannel photodiode based on the avalanche MRS-structure," Proc. SPIE V.1621, p.158 (1991).

[5] Bondarenko, G., Dolgoshein, B., Golovin, V., Ilyin, A., Klanner, R.., Popova, E., “Limited Geiger-mode silicon photodiode with very high gain,” Nucl. Phys. B - Proc. Suppl. 61(3), 347–352 (1998).

[6] Buzhan, P., Dolgoshein, B., Ilyin, A., Kantserov, V., Kaplin, V., et al., “An advanced study of silicon photomultiplier,” ICFA Instrum.Bull. **23**, 28–41 (2001).

[7] Buzhan P., Dolgoshein B., Filatov L., Ilyin A., Kantzerov V., Kaplin V., Karakash A., Kayumov F., Klemin S., et al., "Silicon photomultiplier and its possible applications," Nuclear Instruments and Methods in Physics Research Section A: Accelerators, Spectrometers, Detectors and Associated Equipment 504, 48–52 (2003)

[8] Vinogradov, S., “Probabilistic analysis of solid state photomultiplier performance,” Proc. SPIE - Int. Soc. Opt. Eng. 8375, 83750S–83750S–9 (2012).

[9] Otte, A. N., Dolgoshein, B., Hose, J., Klemin, S., Lorenz, E., Mirzoyan, R., Popova, E.., Teshima, M., “The SiPM — A new Photon Detector for PET,” Nucl. Phys. B - Proc. Suppl. **150**, 417–420 (2006).

[10] Vinogradov, S., “Discrete Amplification Photon Detector (DAPD) evaluation for Optech LIDAR applications”, unpublished (2010).

[11] Son, K. T. and Lee, C. C., "Multiple-Target Laser Rangefinding Receiver Using a Silicon Photomultiplier Array," IEEE Transactions on Instrumentation and Measurement, vol. 59, no. 11, pp. 3005-3011 (2010).

[12] Riu, J., Sicard, M., Royo, S.., Comerón, A., “Silicon photomultiplier detector for atmospheric lidar applications.,” Opt. Lett. **37**(7), 1229–1231 (2012).

[13] Agishev, R., Comerón, A., Bach, J., Rodriguez, A., Sicard, M., Riu, J.., Royo, S., “Lidar with SiPM: Some capabilities and limitations in real environment,” Opt. Laser Technol. **49**, 86–90 (2013).

[14] Agishev, R., Comeron, A.., Gilerson, A., “About the Potential of Lidars with Different Photodetectors Under Daytime Sky Radiation,” Eur. Phys. J. Web Conf. **119**, 25009 (2016).

Ouster Exhibit 2012
IPR2023-01457 - Page 0010

Downloaded From: http://proceedings.spiedigitallibrary.org/ on 05/24/2017 Terms of Use: http://spiedigitallibrary.org/ss/termsofuse.aspx

[15] Adamo, G., Busacca, A., "Time of Flight Measurements via Two LiDAR Systems with SiPM and APD" in *Int. Conf. AEIT-2016*, Capri, Italy, 5-7 Oct. 2016.
[16] Jackson, C., "Laser Range Finding and Imaging LIDAR with Silicon Photomultipliers," in *IWPC - Advanced Radar, Camera, and Laser Sensors for Automated Driving Workshop*, 21 Mar. 2013.
[17] Gnecchi, S., Buckley, S., Bellis, S., Barry, C., and Jackson, C., "SiPM Sensors for ToF Ranging Applications" http://sensl.com/downloads/ds/TN-PhotonicsWest_SensLPOSTER_2016_LiDAR.pdf.
[18] Williams, G. M., Huntington, A. S.., Way, S. W. M., "Probabilistic analysis of Linear Mode vs Geiger Mode APD FPAs for advanced LADAR enabled interceptors," Proc. SPIE 6220, 622008-1 - 622008-14 (2006).
[19] Ullrich, A., and Pfennigbauer, M., "Linear LIDAR versus Geiger-mode LIDAR: impact on data properties and data quality", Proc. SPIE 9832, 983204 (2016)
[20] Zappa, F. and Tosi, A., "MiSPIA: microelectronic single-photon 3D imaging arrays for low-light high-speed safety and security applications", Proc. SPIE 8727, 87270L (2013).
[21] Durini, D., et al., "CMOS Technology for SPAD / SiPM. Results from the MiSPiA Project", in *7th Fraunhofer IMS Workshop on CMOS Imaging from Photon to Camera*, Duisburg, Germany, 20-21 May 2014.
[22] Zou, Yu.; Villa, F.; Bronzi, D.; Tisa, S.; Tosi, A., et al. "Fully CMOS analog and digital SiPMs", Proc. SPIE 9359, 93591B (2015).
[23] Frach, T., Prescher, G., Degenhardt, C., de Gruyter, R., Schmitz, A., Ballizany, R., "The digital silicon photomultiplier — Principle of operation and intrinsic detector performance," 2009 IEEE Nucl. Sci. Symp. Conf. Rec., 1959–1965 (2009).
[24] Frach, T., "Optimization of the digital Silicon Photomultiplier for Cherenkov light detection," J. Instrum. **7**(1), C01112 (2012).
[25] Fishburn, M. W.., Charbon, E., "System tradeoffs in gamma-ray detection utilizing SPAD arrays and scintillators," IEEE Trans. Nucl. Sci. 57(5 PART 1), 2549–2557 (2010).
[26] Seifert, S., et al., "A Comprehensive Model to Predict the Timing Resolution of SiPM-Based Scintillation Detectors: Theory and Experimental Validation", IEEE Trans. Nucl. Sci. **59,** p. 190 (2012)
[27] Seifert, S., van Dam, H. T.., Schaart, D. R., "The lower bound on the timing resolution of scintillation detectors.," Phys. Med. Biol. **57**(7), 1797–1814 (2012).
[28] P. Lecoq, E. Auffray, and S. Gundacker, "Ultimate Time Resolution in Scintillator-based detectors for Calorimetry and Time-of-Flight PET," in Workshop On Picosecond Photon Sensors For Physics And Medical Applications, Clermont-Ferrand, France, March 12-14, 2014.
[29] F. Acerbi et al., "Characterization of Single-Photon Time Resolution: From Single SPAD to Silicon Photomultiplier", IEEE Trans on Nucl. Sci. **61**, Issue: 5 (2014).
[30] Barrett, H. H., Wagner, R. F.., Myers, K. J., "Correlated point processes in radiological imaging," Proc. SPIE **3032**, 110–124 (1997).
[31] Barrett, H. H. and Myers, K. J., [Foundations of Image Science], John Wiley and Sons, New York, 2004.
[32] Vinogradov S., et.al., "Efficiency of solid state photomultipliers in photon number resolution," IEEE Trans. Nucl. Sci. **58** (PART 1), 9–16 (2011).
[33] Vinogradov, S., "Analytical model of SiPM time resolution and order statistics with crosstalk," Nucl. Instruments Methods Phys. Res. Sect. A Accel. Spectrometers, Detect. Assoc. Equip. **787**, 229–233 (2015).
[34] Vinogradov, S., "Performance of silicon photomultipliers in photon number and time resolution," Proc. Sci. **6-9-2**, 1-9 (2015).
[35] Philippov, D., Popova, E., Belyaev, V., Buzhan, P., Stifutkin, A., and Vinogradov, S., "Influence of SiPM single photon timing resolution on coincidence timing resolution with fast scintillator", in *IEEE Nuclear Science Symposium and Medical Imaging Conference (NSS/MIC-2016)*, Strasbourg, France, Oct. 29 - Nov. 6, 2016.
[36] Philippov, D. E., Popova, E. V., Belyaev, V. N., Buzhan, P. Z., Stifutkin, A. A.., Vinogradov, S. L., "Digital Signal Processing for SiPM Timing Resolution," J. Phys. Conf. Ser. **798**(1), 12220 (2017).
[37] Vinogradov, S., "Analytical models of probability distribution and excess noise factor of solid state photomultiplier signals with crosstalk," Nucl. Instruments Methods Phys. Res. Sect. A Accel. Spectrometers, Detect. Assoc. Equip. **695**, 247–251 (2012).
[38] Wagner, W., Ullrich, A., Ducic, V., Melzer, T., Studnicka, N., "Gaussian decomposition and calibration of a novel smallfootprint full-waveform digitising airborne laser scanner", ISPRS Journal of Photogrammetry & Remote Sensing, 60 (2), 100-112 (2006).
[39] Agilent Technologies, "Evaluating Oscilloscope Vertical Noise Characteristics", Application note (2010); http://cp.literature.agilent.com/litweb/pdf/5989-3020EN.pdf

Ouster Exhibit 2012
IPR2023-01457 - Page 0011
Downloaded From: http://proceedings.spiedigitallibrary.org/ on 05/24/2017 Terms of Use: http://spiedigitallibrary.org/ss/termsofuse.aspx